



## Research article

# Impact analysis of dust evolution pattern and determination of key ventilation parameters in highland highway construction tunnels

Jie Liu<sup>a</sup>, Yi Chen<sup>a</sup>, Wanqing Wang<sup>b,\*</sup>, Chenwei Hao<sup>c</sup>, Fei Cai<sup>a</sup>, Liangyun Teng<sup>a</sup>, Xuehua Luo<sup>a</sup>

<sup>a</sup> Faculty of Public Security and Emergency Management, Kunming University of Science and Technology, Kunming, 650093, China

<sup>b</sup> School of Finance, Yunnan University of Finance and Economics, Kunming, 650221, China

<sup>c</sup> Faculty of Land and Resources Engineering, Kunming University of Science and Technology, Kunming, 650093, China

## ARTICLE INFO

**Keywords:**

Highland road tunnel  
Press-in ventilation  
Numerical simulation  
Dust evolution law  
Ventilation parameters

## ABSTRACT

In order to study the influence of ventilation parameters on the ventilation of plateau highway construction tunnels, a highway tunnel construction section in Yunnan is taken as the research background, and Fluent software is used for simulation. The results of the study show that: under the conditions of press-in ventilation, the wind speed in the center of the vortex area in the wind flow field is smaller than the wind speed in the surrounding area, and with the diffusion of the flow field, the average wind speed in the tunnel section gradually decreases, and ultimately stabilizes at the level of 0.5 m/s. After blasting, the dust mass concentration on the return side of the tunnel is higher than that on the duct side. Dust with a particle size of 30  $\mu\text{m}$  or more settled rapidly within 100 m from the boring face, while dust with a particle size of 30  $\mu\text{m}$  or less gradually diffused outward under the action of the wind flow. In the vicinity of the tunnel boring face, reducing the distance from the air outlet to the boring face and increasing the air velocity can improve the dust removal effect. This conclusion can provide theoretical basis and certain guidance for the evolution of dust and dust prevention in the tunnel construction process in plateau area.

## 1. Introduction

Tunnel construction occupies an extremely important position in China's fast-developing modernization, especially in highland areas, where the construction of highway tunnels has always been one of the important tasks in the field of infrastructure. However, dust pollution generated during tunnel construction has always been a serious problem. General particle size greater than 10  $\mu\text{m}$  dust will be filtered and intercepted by the human respiratory organs, and will not be inhaled, but it will cause the construction workers to obstruct the line of sight, visibility inside the cave is easy to cause safety accidents in the project, through the ventilation of the dust will be discharged out of the cave will be the secondary pollution of the surrounding environment. Dust particles particle size in 2.5–10  $\mu\text{m}$  will be adsorbed by the nasal villi, but there are still some particles will enter the respiratory system, resulting in breathing problems, there is a kind of "choking" feeling, the harm to human health is relatively small. The most harmful to the human body is the particle size of 2.5  $\mu\text{m}$  below the fine particulate matter, its particle size is only 1/10 of the diameter of the hair, can be directly through the

\* Corresponding author.

E-mail addresses: [liujie2004@kust.edu.cn](mailto:liujie2004@kust.edu.cn) (J. Liu), [20222239029@kust.edu.cn](mailto:20222239029@kust.edu.cn) (Y. Chen), [zz2127@ynufe.edu.cn](mailto:zz2127@ynufe.edu.cn) (W. Wang), [20222201158@kust.edu.cn](mailto:20222201158@kust.edu.cn) (C. Hao), [20222139004@kust.edu.cn](mailto:20222139004@kust.edu.cn) (F. Cai), [20222239024@kust.edu.cn](mailto:20222239024@kust.edu.cn) (L. Teng), [20222139001@kust.edu.cn](mailto:20222139001@kust.edu.cn) (X. Luo).

<https://doi.org/10.1016/j.heliyon.2024.e33758>

Received 22 March 2024; Received in revised form 25 June 2024; Accepted 26 June 2024

Available online 27 June 2024

2405-8440/© 2024 The Authors. Published by Elsevier Ltd. This is an open access article under the CC BY-NC license (<http://creativecommons.org/licenses/by-nc/4.0/>).

respiratory tract was inhaled into the lungs, and then absorbed by the alveoli for the body's oxygen supply at the same time into the blood circulatory system, greatly reducing hemoglobin for the human body's ability to supply oxygen, often leading to severe human hypoxia fainting, prolonged in the dust-filled conditions will result in the work of Bronchitis, asthma and other respiratory diseases. Inhalable dust is the most harmful to human body, and it is more likely to cause a systemic occupational disease - pneumoconiosis - by lung lesions, and the life expectancy of pneumoconiosis is reduced by 10–15 years per capita.

According to the statistical bulletin of China's health care development, as of 2023, China has reported 11,108 new cases of various types of occupational diseases, including 7577 cases of occupational pneumoconiosis, accounting for nearly 70 % of the total. 9613 deaths due to pneumoconiosis were reported in China in 2023, nearly half of which were due to coal workers' pneumoconiosis, and the proportion of pneumoconiosis among the incumbents was 6.6 %, and the proportion of retired people was as high as 13.7 %. In terms of the current level of medical technology, pneumoconiosis is still a kind of terminal disease that can only be prevented but not cured, so the prevention of pneumoconiosis should do a good job of dust prevention and control, respirable dust prevention and control is both the focus and the difficulty, how to prevent and control the dust in the tunnel and reduce the impact of dust on the personnel and the construction environment is an urgent need to solve the problem.

In terms of tunnel dust, scholars have carried out a large number of studies related to dust transportation and influencing factors. For example, Hou et al. [1] used Eulerian-Lagrangian method to establish a coupled air-dust model, and investigated the dust transport law under different wind conditions. Liu et al. [2] used numerical simulation method combined with on-site measurements, and investigated the diffusion law of dust contamination in tunnels with different suction volumes and different distances of suction openings from cutter faces. Chen et al. [3] analyzed the airflow-dust migration law after the improved ventilation system based on computational fluid dynamics (CFD) to determine the corresponding working parameters. Nie et al. [4] investigated the dust migration behavior during tunnel construction and the influence of ventilation parameters on the airflow and dust migration in the face of tunneling. Hu et al. [5] carried out experiments on the law of dust concentration change with time and the law of blasting dust deposition in the boring face to study the spatial transportation law of dust particles after blasting in long-distance roadway boring. Niu et al. [6] combined numerical calculations and measured data to study the dust generated from the working face of the mine, and obtained the optimal duct diameter, the distance between the air outlet and the tunnel surface, and the height of the duct. Cai et al. [7] conducted numerical simulations by using Computational Fluid Dynamics (CFD) technology in a tunnel set up with different exhaust air volumes and height of the pneumatic tubes above the tunnel floor to evaluate the hybrid ventilation system's of dust suppression performance. If the pressure air volume is kept constant, the diffusion distance of highly concentrated dust decreases with the increase of the exhaust air volume. Jiang et al. [8] performed numerical simulation and analysis of tunnel rock drilling ventilation and dust removal parameters by using Fluent software. Xia et al. [9] established a simulation model of TBM tunneling by using CFD, and investigated the influence of the location of the main ventilation hole on the exhaust air flow field distribution and dust flow characteristics. Kurnia et al. [10] used CFD to simulate the control of toxic and hazardous gases as well as dust particles in tunnels. The optimal ventilation and ventilation parameters were obtained by analyzing the dust removal system. Liu and Wang [11–13] carried out a theoretical analysis of the characteristics of the pressurized ventilation structure to study the distribution pattern of dust in the tunnel, and the results showed that the concentration of dust was larger in the reflux and vortex zones. Torano et al. [14] simulated the evolution of the wind flow and dust in the tunnel using CFD, and got the optimal compression pressure air opening and suction volume, as well as the pressure and inlet air opening distribution locations. Sasmito et al. [15] used four different turbulence models to compare and analyze the airflow characteristics in the tunnel by CFD based software and finally obtained the most suitable model for the tunnel ventilation system. By comparing the various ventilation methods, the best ventilation arrangement system is selected. Liu et al. [16] studied the shield tunnel area south of Line 8 of the Qingdao Transportation International Airport in China as an example, and gave the optimal location of pressure air outlets in the shield tunnel. Sun et al. [17] analyzed the force condition of dust during rock tunnel blasting construction through the theory of gas-solid two-phase flow, and studied the movement and transport law of dust in the tunnel based on the three conservation laws.

In summary, most scholars mainly focus on the parameters of ventilation systems in mines and ordinary tunnels, but the research on the influence of environmental characteristics in high altitude areas on dust migration during tunnel excavation and the determination of key ventilation parameters are not comprehensive enough. Therefore, based on the theory of fluid mechanics, this paper takes a highway tunnel construction section in Yunnan as the research background, uses Fluent fluid simulation software to simulate the dust transport situation after blasting in the construction tunnel according to the actual situation of the plateau where the tunnel is located, and orthogonal synthesis test analysis method on the ventilation distance, ventilation air volume and ventilation height of the three parameters of the tunnel dust quality concentration reduced to the safety threshold to analyze the degree of influence to determine the degree of correlation between the factors and the degree of influence, the relevant conclusions can be for high-altitude areas in the tunnel construction process of the evolution of the dust law and dust prevention and control to provide a theoretical basis and a certain role in guiding.

## 2. Environmental characteristics at high altitudes

The environmental characteristics of high-altitude areas, including the reduction of atmospheric pressure, temperature and air density, have a significant impact on tunnel construction work and the health and safety of workers. These environmental characteristics need to be fully considered when designing the simulation of high-altitude tunnels to ensure the credibility of the simulation results.

### 2.1. The effect of altitude on atmospheric pressure

There is a close relationship between altitude and atmospheric pressure at high altitudes. As the altitude increases, the thickness of the atmosphere decreases, and the density and pressure of the gas molecules decrease [18]. According to the International Standard Atmospheric Model (ISAM), the atmospheric pressure decreases by about 10 % for every increase in altitude of about 1000 m.as shown in Table 1. The relationship between the two is expressed as follows:

$$P_z = 101325 \times \left(1 - \frac{h}{44329}\right)^{5.2555876} \tag{1}$$

Among :  $P_z$  is the atmospheric pressure at an altitude of  $Z$ ,  $P_a$ ;  $Z$  is the altitude, m.

Lower atmospheric pressure can have a number of effects on tunnel construction. First, low atmospheric pressure leads to a reduction in air density, which reduces oxygen content. This can pose a challenge to workers performing physical labor and breathing at high altitudes. Secondly, as the atmospheric pressure decreases, the gas mobility in the air also decreases, which may have an impact on engineering measures such as ventilation and dust removal.

### 2.2. The effect of altitude on temperature

As the distance from the ground to the atmosphere increases with increasing altitude, the absorption of solar radiation and heating of the earth’s surface decreases, resulting in a decrease in temperature. According to climatological observations and studies, the average temperature shows a decreasing trend with increasing altitude [19]. For every 1 km increase in altitude, the average temperature decreases by about 5 °C.as shown in Table 2. This can be calculated according to the following equation:

$$t_z = t_A - \frac{g_t \cdot \Delta Z}{100} \tag{2}$$

Among:  $t_z$  is the temperature at elevation  $z$ , °C;  $t_A$  is the temperature of the adjacent weather station, °C;  $g_t$  is the temperature gradient, 0.5–0.7 °C/100 m;  $\Delta Z$  is the difference between the altitude at the altitude  $Z$  and the adjacent weather station, m.

When tunneling at high altitude, the decrease in temperature may bring some problems to the project. Firstly, low temperatures may affect the workers’ body sensation and physical functions, and increase labor intensity and work pressure. Secondly, the low temperature environment may adversely affect the performance of equipment and materials, such as increased viscosity of lubricants and embrittlement of materials.

### 2.3. The effect of altitude on air density

Air is thin at high altitudes and the density of gases will decrease gradually with altitude. Ideal gas molecules have mass and no volume, and have no interaction with other molecules. Under normal temperature and low pressure conditions, air can be approximated as an ideal gas. According to the ideal gas equation of state.  $PV = mRT/M$  can be deduced from the formula for the density of air at different temperatures and pressures:The air densities corresponding to different altitudes are shown in Table 3.

$$\frac{\rho_H}{\rho_0} = \frac{P_H}{P_0} \cdot \frac{T_0}{T_H} \tag{3}$$

Among ,  $\rho_0$  is the air density under standard conditions, 1.293 kg/m<sup>3</sup>;  $\rho_H$  is the density of the air at altitude  $H$ , 1.293 kg/m<sup>3</sup>;  $P_H$  is the atmospheric pressure at altitude  $H$ ,  $P_0$ ;  $T_H$  is the absolute temperature at altitude  $H$ , °C.

A low-oxygen environment can adversely affect the health and work capacity of tunnel construction workers. When performing strenuous physical labor at high altitude, workers may experience shortness of breath, fatigue and dizziness due to reduced oxygen supply. This poses a potential threat to work efficiency and worker safety.

## 3. Simulation overview and calculation settings

### 3.1. Discrete phase model

Gas-solid two-phase flow in tunnel ventilation systems conforms to the discrete-phase model in numerical simulations. The discrete-phase model is a kind of Euler-Lagrange model, which is used to describe the gas-phase flow field and the mutual motion between particles.

**Table 1**  
Atmospheric pressure corresponding to different altitudes.

Altitude/m	0	1500	3000	4500	6000	Expression
Pressure/Pa	101325	84547	70093	57708	47158	$P_z = 101325 \times \left(1 - \frac{h}{44329}\right)^{5.2555876}$

**Table 2**  
The temperature corresponding to different altitudes.

Altitude/m	0	1500	3000	4500	6000	Expression
Temperature/K	288.2	278.4	268.7	258.9	249.2	$t_z = t_A - \frac{g_x \cdot \Delta Z}{100}$

**Table 3**  
The density of air at different altitudes.

Altitude/m	0	1500	3000	4500	6000	Expression
Density of air/(kg·m <sup>-3</sup> )	1.226	1.059	0.909	0.777	0.660	$\frac{\rho_H}{\rho_0} = \frac{P_H}{P_0} \cdot \frac{T_0}{T_H}$

The equation :

$$\frac{du_p}{dt} = F_D(u - u_p) + \frac{g_x(\rho_p - \rho)}{\rho_p} + F_x \tag{4}$$

Among:  $u_p$  is the discrete phase velocity, m/s;  $F_D(u - u_p)$  is the trailing force per unit mass of the discrete phase, N;  $u$  is the fluid phase velocity, m/s;  $g_x$  is the acceleration of gravity in the X direction, m/s<sup>2</sup>;  $\rho_p$  is the discrete phase density, kg/m<sup>3</sup>;  $F_x$  is other forces, N.

$$F_D = \frac{18\mu}{\rho_p d_p^2} \frac{C_D Re}{24} \tag{5}$$

Among:  $C_D$  is the drag force coefficient;  $d_p$  is the particle diameter, m;  $Re$  is the relative Reynolds number (particle Reynolds number).

$$Re = \frac{\rho d_p |u_p - u|}{\mu} \tag{6}$$

$$C_D = a_1 + \frac{a_2}{Re} + \frac{a_3}{Re^2} \tag{7}$$

Among:  $a_1, a_2, a_3$  is constant.

### 3.2. Numerical simulation model of high-altitude tunnel

#### 3.2.1. Geometry and meshing

The tunnel site of this paper is located in the mountainous area of Yunnan Plateau, in the connection line of Yuanyang Airport of Yuanyang-Luchun Expressway, which is a separated tunnel, with a cumulative total length of 3671.56 m in left and right widths, belonging to the extra-long tunnel, with an elevation of 2639.6 m. The climate belongs to the type of subtropical mountain monsoon, with the average rainfall for many years being from 1450.89 mm to 2108.99 mm respectively. The climate in mountainous areas is variable, with an annual average temperature of 16.4 °C, a maximum temperature of 43.5 °C and a minimum temperature of 3.7 °C. The dry season is from November to April, and the climate in the tunnel site is mild, with rainy and foggy days, sometimes with frost, and the precipitation is 1779.99 mm. The tunnel shows obvious geographical features of the Yunnan-Guizhou Plateau, which is typical of high-altitude highway tunnels, and is therefore selected as the study object.

In order to realize the effect of numerical simulation reacting to the actual situation on the site, the physical model with the main hole of the high-altitude tunnel as the research object is established according to the introduction of the project overview and the reference of the on-site construction data. Due to the complexity of the tunnel construction process, which involves many links, it is difficult to completely reproduce the details of the tunnel construction site, so the numerical simulation simulation model is simplified and assumptions: the air flow rate in the tunnel space is small, assuming that its density is unchanged, and the air flow in the tunnel space is regarded as an incompressible flow; the wind flow from the pressurized wind turbine into the tunnel is fresh air, which does not entrain other pollutants, and dust is all generated by the Palm surface blasting, tunnel blasting dust from the palm surface uniform spray, assuming that all the dust generated in the instant of blasting, as an instantaneous source of pollution; dust in the tunnel are from the blasting process of tunneling face, dust particles of small size, and for the spherical particles, ignoring the interaction between the particles, and only consider the gravity of dust, buoyancy, and the airflow drag resistance.

Based on the above assumptions, SpaceClaim was used to model the tunnel at a scale of 1:1. The inner radius of the main tunnel is 5.5 m, the total width is 11.0 m, the height is 7.1 m, and the sectional area of the tunnel is 64.83 m<sup>2</sup>. On the left side of the tunnel, a 75\*2 KW counter-rotating axial flow ventilator is connected to a Φ1.2 m ventilating hose to ventilate the tunnel according to the press-in ventilation method, and the site adopts the press-in ventilation, the site adopts the press-in type ventilation, the air outlet of the wind pipe is 35 m away from the face of the excavation, and the diameter is 1.2 m, and the velocity of the air supply is 12 m/s, and the position of the wind pipe is suspended on the side wall of the tunnel, and the center of the wind pipe is 4 m away from the ground

height. There is a secondary lining trolley, whose length is 12 m, and the length range is 200 m away from the face of the excavation is selected for the study. At 168 m from the boring face is the secondary lining cart, the length of which is 12 m, and 200 m from the boring face is selected as the research object, the model is imported into ANSYS Workbench, and ANSYS Mesh is used to mesh the model, so as to obtain the physical model of the tunnel and the mesh as shown in Fig. 1.

### 3.2.2. Mesh independence test

When simulating the wind flow field and dust diffusion using computational fluid dynamics, the quality of the mesh will directly affect the efficiency and accuracy of the simulation, so it is necessary to verify the mesh independence of this physical model. ANSYS Mesh software is utilized to mesh the physical model, generating three meshes with different qualities of coarse mesh (Mesh A), medium mesh (Mesh B), and fine mesh (Mesh C), as shown in Table 4.

Wind flow is the main factor governing the dust diffusion pattern and dust pollution effect, so the wind speed distribution along the tunnel at 1.5 m height of the human breathing zone is selected as the grid independence verification parameter. The wind flow field distribution under different grids is obtained, as shown in Fig. 2.

As can be seen from Fig. 2, the calculation results of the three grids are similar, and the wind speed shows the trend of increasing and then decreasing, and the peak of wind speed is obtained near the outlet of the air duct. There is only a slight difference in the wind speed at 10–120 m from the face. This shows that although the quantity and quality of the grids divided by the three schemes are different, they have realized the grid independence. In this paper, a medium quality mesh (Mesh B) is selected for the study.

The results of the mesh quality check of the middle mesh (Mesh B) are shown in Fig. 3, where the horizontal coordinate is the mesh quality and the vertical coordinate is the number of meshes; the meshes with a mesh quality greater than 0.5 accounted for 99.98 % of all the meshes, and the mesh types are reasonable, with a suitable degree of sparsity for subsequent numerical simulation calculations.

### 3.3. Boundary conditions and parameter settings

After importing the model into Fluent, initial boundary conditions need to be set for the geometric model. The tunnel opening is the pressure outlet, the outlet of the wind turbine is the velocity inlet, and the wind velocity of the wind turbine is positive; the tunnel boring face is the dust ejection source; and the rest of the interfaces are set as the wall boundaries. There are two kinds of materials in the tunnel, continuous phase (air) and discontinuous phase (dust particles), and the DPM (Discrete Phase Model) model can be used to better calculate the coupling problem of dust particles moving in the air [20], and the specific model parameters are set as shown in Table 5.

## 4. Analysis of simulation results

### 4.1. Analysis of dust pollution effects after blasting

#### 4.1.1. Distribution law of wind current flow field

Ventilation is the simplest and most commonly used method to control dust concentration during tunnel construction. The distribution of the wind flow field in the tunnel directly affects the propagation of dust after blasting operations. Therefore, it is of great significance to study the distribution law of wind flow field in tunnels. In this paper, first of all, the wind flow field in the construction tunnel was numerically simulated, and the distribution of the wind flow field in the tunnel as well as the trend of the wind speed along the central axis of the tunnel were obtained from the simulation results, which are shown in Fig. 4(a) and (b). In the figure, X direction is the direction of tunnel width, Y direction is the direction of tunnel height, and Z direction is the direction of tunnel length.

From Fig. 4, the wind flow shot out of the air outlet of the press-in type wind pipe can reach the palm face, indicating that it is reasonable to set the distance from the air outlet of the wind pipe to the palm face at 35 m. Within the effective range of the air outlet jet, it helps to remove the dust after blasting operations. Since the press-in wind pipe is in close contact with the side wall of the tunnel, the fresh wind flow shot out of the outlet flows along the right arch of the tunnel, forming an obvious phenomenon of wall-attached jet. After the fresh wind jet is shot out of the outlet, the fresh wind jet will quickly reach the palm face, and the direction of the wind flow

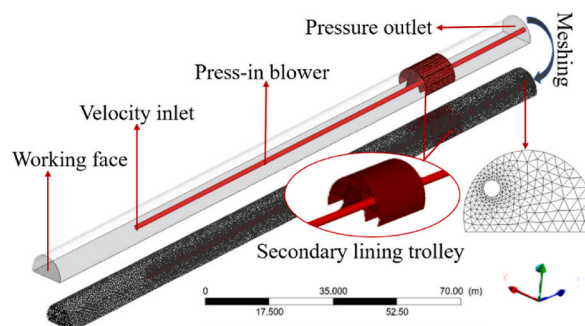
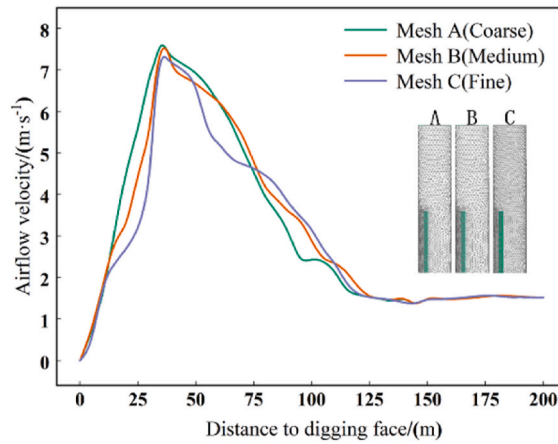


Fig. 1. Tunnel physical modelling and meshing.

**Table 4**  
Grid division.

Mesh name	Unit size/m	Mesh nodes	Number of meshes	Mesh quality
Mesh A	1.2	1214355	1275046	0.32-1
Mesh B	1.0	1218563	1321659	0.39-1
Mesh C	0.8	1326838	1413728	0.36-1



**Fig. 2.** Variation of wind speed on different grids.

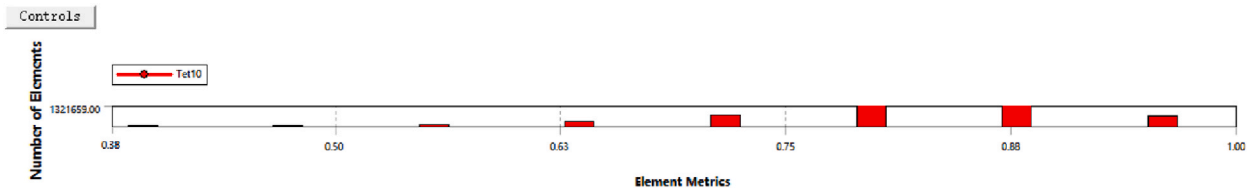


**Fig. 3.** Grid quality distribution.

**Table 5**  
Parameter settings of the model.

Parameter settings	Parameter	Parameter settings	Parameter
Injection Type	Surface	Energy	OFF
Diameter Distribution	Rosin-Rammler	Air	1.023 kg/m <sup>3</sup>
Min.Diameter	1 × 10 <sup>-6</sup> m	Temperature	298K
Max.Diameter	1 × 10 <sup>-4</sup> m	Pressure	82500pa
Mid.Diameter	1.2 × 10 <sup>-5</sup> m	Solver	Transient Time
Spread Parameter	1.93	Viscous	Realizable k-ε
Total Flow Rate	0.02 kg/s	Discrete Phase Model	ON
Lengh Scale	0.01	Interaction with Continuous Phase	ON
Max Number of Step	5000	Turbulent Dispersion	Stochastic Tracking

changes under the influence of the palm face, on the center axis, within the range of 0~35 m from the boring face, the speed of the wind flow gradually increases, and the highest wind speed reaches 6.8 m/s, and within the range of 35~55 m from the boring face, the speed of the wind flow slows down gradually, and the highest wind speed reaches 2.1 m/s, and then gradually tends to stabilize.

When the new wind jet arrives at the face of the palm, under the influence of the face of the palm, the wind flow is directed to the left side of the tunnel, due to the spatial limitation of the tunnel boring face and the continuity of the wind flow, the direction of the impact-adhesive wind flow changes, and the free jet flows in the opposite direction outward, thus forming the return flow area. With the increase of distance from the palm face, the return wind gradually spreads to the inlet side, and eventually distributed in the whole tunnel space. Due to the large wind speed at the outlet of the wind pipe, near the outlet, part of the return air is attracted by the jet at the outlet to flow to the face of the palm, and the other part of the return air continues to flow in the direction of the tunnel entrance. Due to the interaction between the two, a vortex area is formed between the jet area and the return area, and the vortex area is very

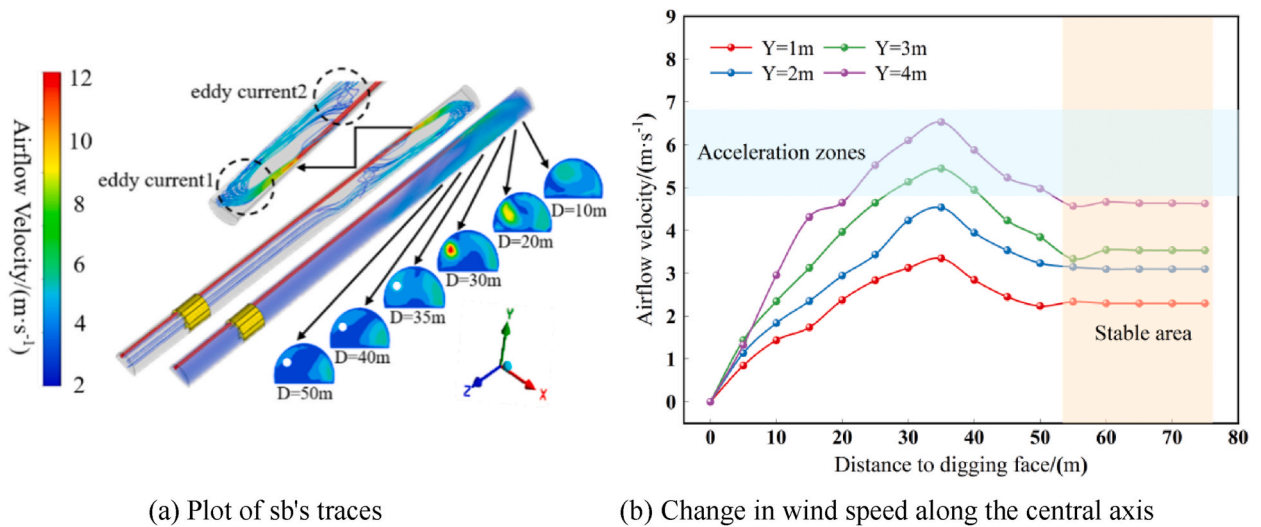


Fig. 4. Distribution of wind current fields.

easy to form a collection of dust, and the concentration of dust is relatively high in this area.

4.1.2. Characterisation of dust deposition after blasting

A large amount of dust is generated after blasting in a boring face, and it is difficult to clearly analyze the transport of dust particles after blasting under pressurized ventilation conditions, relying only on the interaction between airflow and dust. Internationally, solid suspended particles with a particle size  $<75 \mu\text{m}$  are defined as dust, and in dust removal technology, according to its particle size, it can be divided into total suspended particulate matter (TSP) with an aerodynamic diameter of less than or equal to  $100 \mu\text{m}$ , and respirable particulate matter (PM10) with an aerodynamic diameter of less than or equal to  $10 \mu\text{m}$ . Therefore, this paper selected dust particles within the range of  $1 \sim 100 \mu\text{m}$  to be investigate the settling pattern of larger dust particles and derive the range of dust particle sizes at different locations within the tunnel environment.

Dust filled the entire tunnel 6–8 min after the start of ventilation. Therefore, the simulation of tunnel ventilation after blasting was carried out with a time interval of 60s. The time period of 1~6 min after blasting was selected, and the results of dust particle size diffusion with time and distance in the tunnel were obtained, as shown in Fig. 5. After the ventilation reached 10 min, the particle size distribution of dust in different sections of the tunnel, as shown in Fig. 6.

From Fig. 5, after blasting, the dust in the tunnel space is affected by the wind flow, and the dust mass concentration near the boring face gradually decreases with the passage of time. After 60s of ventilation, the dust spreads to 1/4 of the tunnel, and the dust particles are more aggregated and the concentration is higher; after 180s of ventilation, the dust spreads to 1/2 of the tunnel, and at this time, the dust with a particle size of  $30 \mu\text{m}$  or more gradually settles to the ground and is arrested, and the amount of dust floating in the air is gradually reduced. After 360s of ventilation, the dust has spread to the exit of the tunnel, and most of the dust particles in the tunnel are below  $30 \mu\text{m}$ .

From Fig. 6, the particle size range of the dust particles in the tunnel decreases with the increase to the boring face. Dust particles

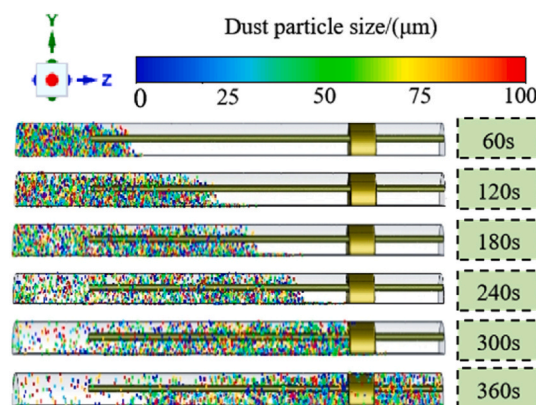


Fig. 5. Dust particle size dispersion.

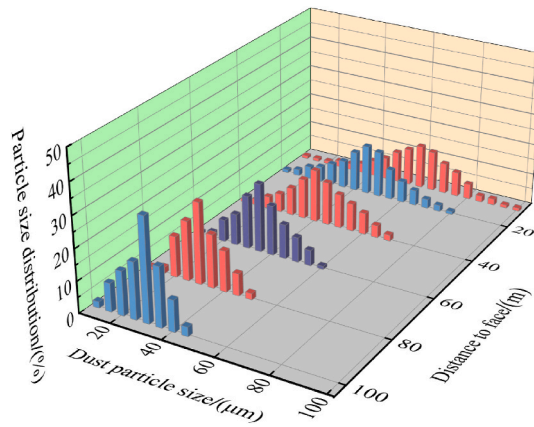


Fig. 6. Dust particle size distribution.

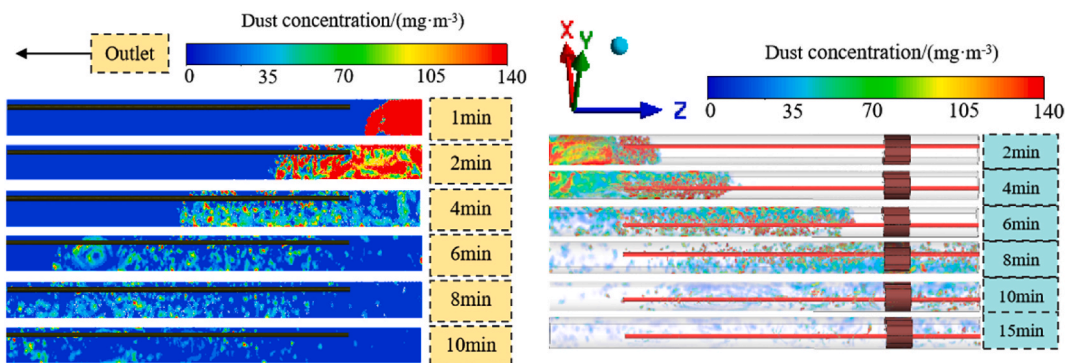
with a diameter of more than 30  $\mu\text{m}$  gathered and settled on the return side, while dust particles with a diameter of less than 30  $\mu\text{m}$  were transported out of the tunnel with the wind flow. After 360s of ventilation, in the range of 100 m in front of the tunnel, most of the dust particles with a diameter of more than 30  $\mu\text{m}$  have basically finished settling, while the dust particles with a diameter of less than 30  $\mu\text{m}$  continue to diffuse towards the tunnel exit direction.

4.1.3. Dust transport characterization after blasting

In order to analyze the coupled diffusion characteristics of airflow and dust in the tunnel, The overall distribution of dust in tunnels and the transport of dust in the breathing zone at a height of 1.5 m were investigated., as shown in Fig. 7. In addition, In order to be able to gain insight into the evolution of dust mass concentration with time at different cross-sectional locations, it is known from Fig. 7(a) that the dust in the first 60 m of the tunnel is relatively dense while the dust in the next one is relatively dispersed, therefore, a cross-section is selected for every interval of 20 m in the first 60 m, and a cross-section is selected for every interval of 40 m thereafter, so as to more comprehensively grasp the interaction between the airflow and the dust. Laws. That is to say, six cross sections were selected from the digging face of 20, 40, 60, 100, 140, 180 m, etc., and the curves of the dust mass concentration with time on each cross section were obtained, as shown in Fig. 8.

From Fig. 7, Under the action of airflow traction resistance, the dust particles move toward the outside of the tunnel, and after 3–4 min of ventilation, the dust spreads to the middle of the tunnel, while after 6–8 min of ventilation, the dust spreads to the tunnel exit. With the increase of ventilation time, the dust mass concentration near the boring face gradually decreases, and under the effect of high-speed jet and return flow, the dust mass concentration on the return side of the tunnel is larger than that on the duct side, and the diffusion of dust on the return side near the wall is relatively slow.

From Fig. 8, With the increase of ventilation time, the distribution range of dust gradually increased, and the area with dust quality concentration less than 10  $\text{mg}/\text{m}^3$  also gradually expanded. The dust quality concentration of each cross-section shows a trend of rapid increase and gradual decrease, the farther away from the boring face, the dust quality concentration increases to the peak and decreases more slowly, and the peak value of each cross-section decreases gradually, the cross-section dust quality concentration at the distance of 20 m from the boring face is 139.32  $\text{mg}/\text{m}^3$ , and at the distance of 180 m from the boring face is 33.18  $\text{mg}/\text{m}^3$ ; after 15 min



(a) Breathing zone height Y=1.5m dust migration

(b) Overall dust distribution in the tunnel

Fig. 7. Dust concentration distribution over time.



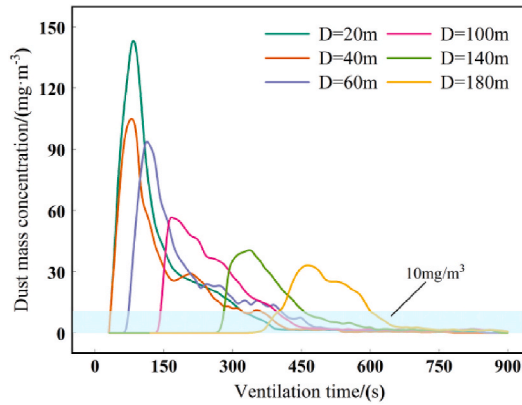


Fig. 8. Variation of dust concentration by cross-section.

of ventilation, the dust quality concentration in the tunnel are all increased gradually. After 15 min of ventilation, the dust mass concentration in the tunnel was reduced to less than 10 mg/m<sup>3</sup>, reaching the safety threshold.

4.2. Effect of wind speed on dust suspension time

In order to study the influence of the wind speed of the wind pipe on the transportation law of dust particles in the tunnel, the distance from the wind pipe outlet to the boring face was determined to be 35 m, and the wind speed of the wind pipe outlet was selected to be 6 m/s, 8 m/s, 10 m/s, 12 m/s, and 14 m/s for the study, respectively. In order to have a more comprehensive understanding of the safety conditions in the tunnel, the simulation results after 360s of ventilation were selected for the study, and the distributions of the dust particle size, the mean value of the concentration along the section, and the dust mass concentration in the tunnel were obtained, as shown in Figs. 9–11.

From Fig. 9, During the same ventilation time, the peak dust concentration gradually increases with increasing wind speed and gets closer to the tunnel exit. This increase may be due to the fact that the diffusion of dust decreases with the increase of wind speed; at the same time, the gradual approach of the peak to the tunnel exit is due to the fact that the increase of wind speed leads to an increase in the rate of the overall transportation of dust to the tunnel exit.

From Fig. 10, Due to the wrapping effect of the wind flow, the dust quality concentration can be reduced to a safe value in a certain area near the digging face. Moreover, the greater the wind speed, the greater the safety range. When the wind speed is 6 m/s, the dust quality concentration in the tunnel is higher than 2 mg/m<sup>3</sup>; however, when the wind speed is increased to 14 m/s, the dust quality concentration in the tunnel within 60 m near the face of the tunnel is lower than 2 mg/m<sup>3</sup>, which reaches the safe concentration. However, when the wind speed is too high, it will cause the dust with small particle size to remain suspended at 180 m from the working face, and it is difficult to realize the settlement.

From Fig. 11, At different wind speeds, there were differences in the velocity of dust discharged to the outside of the tunnel. In the same ventilation time, when the wind speed is 6 m/s, the dust is not diffused to the middle of the tunnel, and when the wind speed is 12 m/s and 14 m/s, the dust is able to be diffused to the tunnel exit, but when the wind speed is 14 m/s, the dust with a particle size of less than 30 μm continues to be suspended in the vicinity of the cart due to the excessive wind speed, which reduces the dust removal effect. Therefore, the higher the wind speed at the end of the wind turbine, the faster the dust is discharged from the tunnel, but the excessive wind speed at the wind turbine exit will cause secondary dust lifting in the tunnel; and in the area near the boring face, the dust quality concentration decreases with the increase of wind speed. Therefore, moderately increasing the air supply helps to dilute the dust

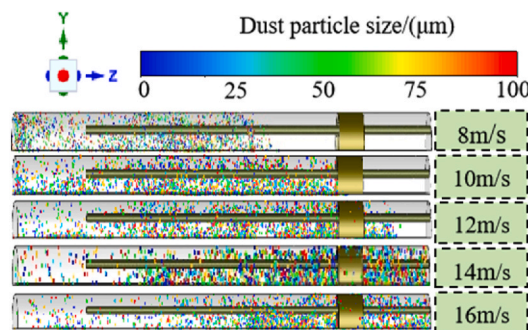


Fig. 9. Dust particle size distribution.

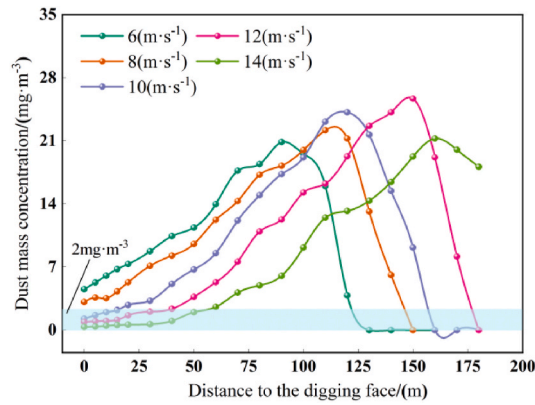


Fig. 10. Change in dust concentration.

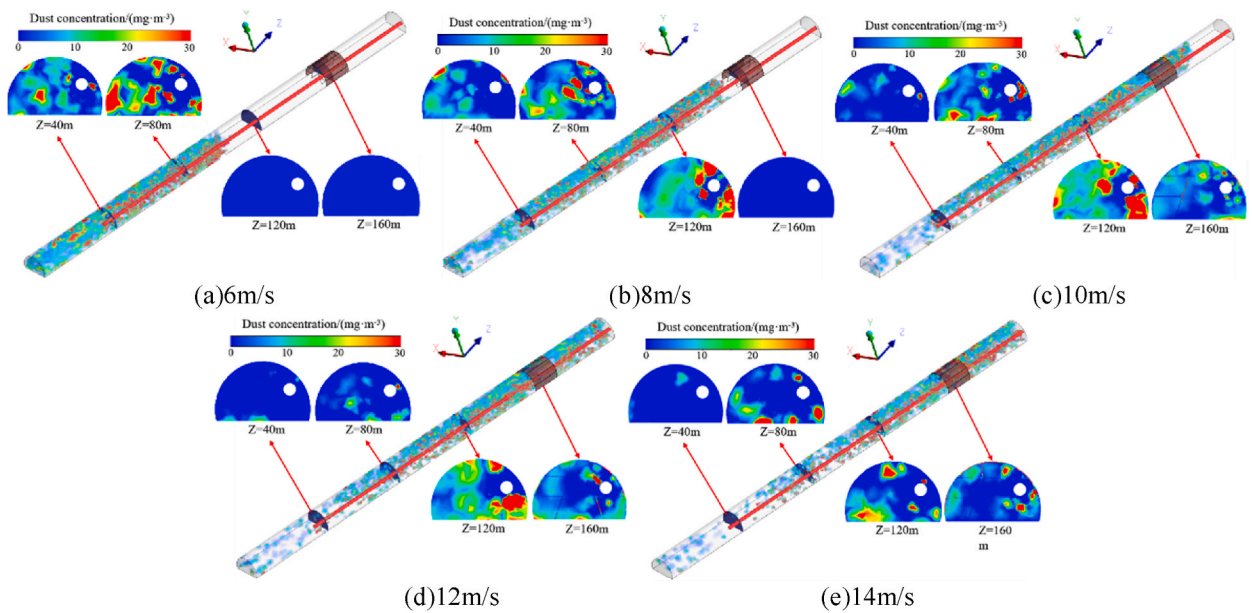


Fig. 11. Dust concentration distribution along the section.

quality concentration and accelerate the discharge and settlement of dust particles.

#### 4.3. Effect of duct distance on dust suspension time

In order to study the influence of the distance from the outlet of the tunnel wind pipe to the boring face on the transportation law of dust particles, the wind speed was determined to be 12 m/s, and the wind pipe was set up at 25, 30, 35, 40 and 45 m away from the boring face for the study, respectively. Simulation obtained ventilation 360s when the dust particle size in the tunnel, the average value of the concentration along the tunnel section and the distribution of dust mass concentration in the tunnel as shown in Figs. 12–14.

From Fig. 12, the larger the distance of the wind turbine outlet from the boring face, the more significant the concentration difference between the two sides of the tunnel, when the distance is 45 m, the highest dust quality concentration in the tunnel is 28.16 mg/m<sup>3</sup>, when the distance is 25 m, the highest dust quality concentration in the tunnel is 13.65 mg/m<sup>3</sup>, and the maximum difference is 14.51 mg/m<sup>3</sup>. With the increase of ventilation distance, the dust mass concentration in the vortex region gradually increases, while the dust concentration in the transition and stabilization regions gradually decreases. The reason for this phenomenon may be due to the fact that the farther the outlet of the duct is from the face of the boring, the stronger the interaction between the jet and the return flow is, resulting in an increase in the vortex range. This results in a smoother dust emission in the area near the boring face. As a result, the dust mass concentration in this region increases with the distance from the duct outlet to the boring face during the same ventilation time, while the opposite trend is observed in the section from the duct to the tunnel exit.

From Figs. 13 and 14, after 360s of ventilation, the dust mass concentration on the wind tunnel side was significantly higher than

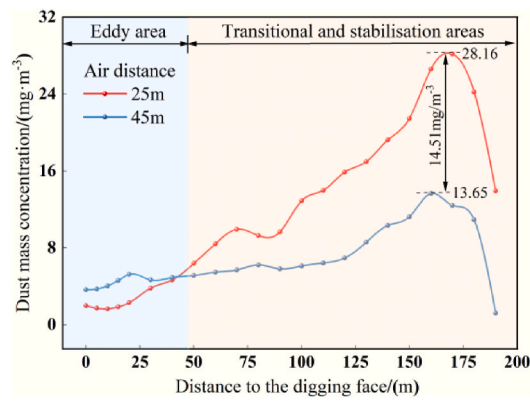


Fig. 12. Change in dust concentration.

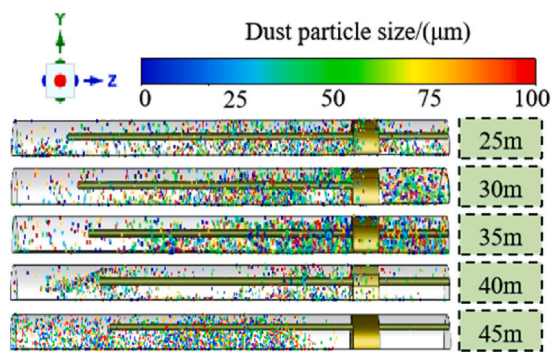


Fig. 13. Dust particle size distribution.

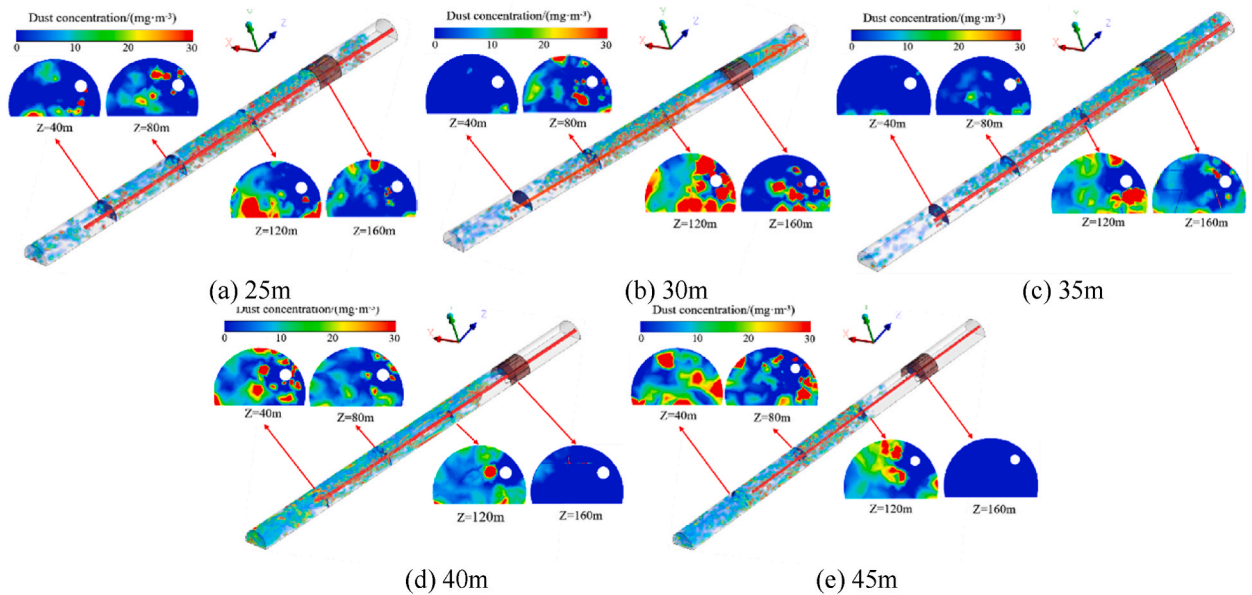


Fig. 14. Distribution of dust concentration along the course section.

that on the return side due to the wind flow. Under the same ventilation time, when the distance is more than 40 m, the wind speed is too small due to air resistance, and the dust in the tunnel fails to diffuse to the outlet, thus failing to achieve the dust removal effect; when the distance is lower than 30 m, the distance is too small, which will result in multiple vortex zones, causing the dust to pile up in

the cart and thus reducing the dust removal effect. The farther the distance from the outlet to the digging face, the more the wind speed of the jet is attenuated under the action of air resistance, resulting in the smaller wind speed of the return flow. This further leads to a larger area of return flow action, making the jet and return flow more dispersed. Appropriately shortening the ventilation distance between the air outlet of the wind pipe and the digging face is conducive to diluting the dust quality concentration near the digging face, but because the distance is too small, it will result in multiple vortex zones, which will cause the dust to pile up at the cart and thus reduce the effect of dust removal, so the air pipe outlet should not be less than 25 m from the digging face, therefore the ventilation distance between the air outlet of the wind pipe and the digging face can be appropriately shortened to improve the environment of the blasting operation.

#### 4.4. Orthogonal-analysis

In order to optimize the tunnel ventilation and dust removal parameters, orthogonal experimental synthesis analysis was used to analyze the extent to which the three parameters, ventilation distance, ventilation airflow, and ventilation height, are required to influence the reduction of dust mass concentration in the tunnel to a safe threshold value. Orthogonal comprehensive analysis is a commonly used experimental design method, which is mainly used to study the influence of multiple factors on the system, and to reduce the number of experiments and obtain the best results through a reasonable experimental design.

In order to show more directly the effect of each factor and each level on the experimental results as well as to reduce the workload, three factors and three levels for each factor were selected based on the results of the numerical simulation analysis, as shown in Table 6.

Since 3 levels are taken for each factor and in order to save the number of experiments, the smaller table should be preferred, i.e.,  $L_9$  ( $3^4$ ) is selected. Where "L" is the code name of the orthogonal table; "9" means that this table has 9 rows and 9 experiments need to be arranged using this table; "3" means that 3 levels are arranged for each factor; "4" means that this table has 4 columns. Since there are only 3 factors, an empty column is added here. The table header design is shown in Table 7.

In order to avoid systematic errors, the method of checking the table of random numbers is used to determine the correspondence. In order not to make the notation too complicated, it is assumed that levels  $A_1, B_1, C_1$ , are represented by number 1, levels  $A_2, B_2, C_2$ , by number 2, and levels  $A_3, B_3, C_3$ , by number 3. The distance of dust diffusion under ventilation for 180s as a percentage of the total length of the tunnel was taken as the test result  $y_i$  ( $i = 1, 2, \dots, n$ ), and the order of the test was determined by drawing lots, and the results were labeled on the last column. Table 8 of the experimental program is established as follows.

From the ANOVA table, it can be seen that the role of factor B is not significant, and it can be considered that altitude is a secondary factor affecting the transportation of tunnel dust. The role of factor A is significant and the role of factor C is more significant. From the calculation Table 9,  $K_{12} > K_{13} > K_{11}$  .  $K_{32} > K_{33} > K_{31}$ . Therefore, the better level is  $A_2$  and  $C_2$ , and the better factor level collocation is  $A_2B_1C_2$ . This indicates that the distance of the air duct from the boring face is the main factor that affects the time needed to reduce the dust quality concentration to a safe value; the air velocity of the air duct air supply can also have an important effect on the diffusion of dust in the tunnel; Altitude also has a relatively limited effect in terms of dust deposition, etc., but it is not negligible.

In order to improve the construction environment after tunnel blasting, first of all, we can consider moderately shortening the distance from the outlet of the wind pipe to the boring face, which is a feasible and highly operational means. At the same time, you can also increase the wind speed of the wind pipe outlet to accelerate the emission of dust. On the basis that the high-altitude environment itself helps the dust to settle, the above measures can be taken to reduce the ventilation time to meet the safety standards.

### 5. Conclude

- (1) Under the conditions of press-in ventilation, the distribution of the air flow field in a high-altitude tunnel can be divided into three regions: vortex region, transition region and stabilization region. In this scenario, the high-speed fresh air and the air around the tunnel transfer momentum under the action of shear force, which leads to the gradual expansion of the jet cross section. The wind speed in the center of the vortex zone is less than that in the surrounding area. As the flow field spreads, the average wind speed in the tunnel cross section gradually decreases and eventually stabilizes at a level of about 0.5 m/s.
- (2) After blasting, the dust particles are driven by the wind flow to the outside of the tunnel, in which the dust mass concentration on the return side of the tunnel is higher than that on the duct side. Dust particles with a diameter of 30  $\mu\text{m}$  or more generated by blasting settled rapidly within 100 m from the face of the tunnel, while dust particles with a diameter of 30  $\mu\text{m}$  or less were suspended in the tunnel space and gradually diffused outward under the action of the wind flow. In addition, the diameter of the dust particles decreases with the increase of the distance from the boring face.

**Table 6**  
Numerical simulation parameter results.

factor	level		
	1	2	3
Air velocity ( m/s ) A	10	12	14
Altitude ( km ) B	1.5	3.0	4.5
Ventilation distance ( m ) C	30	35	40

**Table 7**  
Header design.

Factor	A	B	C	Blank
Number	1	2	3	4

**Table 8**  
Pilot program table.

	A	B	C	Test results yi (%)
	1	2	3	
1	1(10 m/s)	1(1.5 km)	1(30 m)	38
2	1	2(3.0 km)	2(35 m)	54
3	1	3(4.5 km)	3(40 m)	31
4	2(12 m/s)	1	2	64
5	2	2	3	42
6	2	3	1	62
7	3(14 m/s)	1	3	49
8	3	2	1	57
9	3	3	2	53

Following the data in Table 8, the observed values of each statistic were calculated and listed in Calculation Table 9 below.

**Table 9**  
Calculation table.

	A	B	C	Blank	yi
	1	2	3	4	
1	1	1	1	1	38
2	1	2	2	2	54
3	1	3	3	3	31
4	2	1	2	3	64
5	2	2	3	1	42
6	2	3	1	2	62
7	3	1	3	2	49
8	3	2	1	3	57
9	3	3	2	1	53
K <sub>j1</sub>	123	141	135	144	K = 450
K <sub>j2</sub>	183	165	171	153	P = 22500
K <sub>j3</sub>	144	144	114	153	Q = 23484
Q <sub>j</sub>	23118	22614	22734	22518	
S <sub>j</sub> <sup>2</sup>	618	114	234	18	S <sub>T</sub> <sup>2</sup> = 984

From the above table we know that  $S_A^2 = S_1^2, S_B^2 = S_2^2, S_C^2 = S_3^2, S_E^2 = S_4^2$ , the degree of freedom of  $S_A^2, S_B^2, S_C^2$  are all 2,  $S_T^2$  is 8 and  $S_E^2$  is 2. According to the rule of calculating the analysis of variance (ANOVA), the ANOVA Table 10 is listed as follows.

**Table 10**  
The ANOVA.

Source of variance	Square sum	Degrees of freedom	Mean square	F	Significance
Factor A	618	2	309	34.33	*
Factor B	114	2	57	6.33	
Factor C	234	2	117	13.00	(*)
Inaccuracies	18	2	9		
Sum	984	8			

The symbols "\*" and "(\*)" in the significance column of the ANOVA table indicate, respectively, that at the significance level  $\alpha = 0.05, 0.10$  the test results are a rejection of the hypothesis, and it can be assumed that the factor is not a major factor in the problem under examination. The critical values at this point are,  $F_{0.90}(2,2) = 9.00$ ,  $F_{0.95}(2,2) = 19.00$ ,  $F_{0.99}(2,2) = 99.00$ .

- (3) Near the working face of the construction tunnel boring, appropriately shorten the distance between the working face of the boring and increase the wind speed of the air supply, which can improve the effect of dust removal. The ventilation effect is best when the wind speed of the wind pipe outlet is 12 m/s, the distance from the boring face is 35 m, and the ventilation is 15 min. From the gray correlation analysis, it is concluded that the distance of the air duct from the face has the greatest influence on the time needed to reduce the dust quality concentration to the safe value, and the air velocity of the air duct is the second largest influence. This conclusion can provide a theoretical basis and certain guidance for the evolution of dust and dust prevention

during tunnel construction in high altitude areas. Dust of different particle sizes, the weight of influencing factors, combined with the conclusion of the.

## Funding

This research was funded by Yunnan Fundamental Research Projects (grant number 202201AU070110), Yunnan University of Finance and Economics Scientific Research Fund Project (grant number 2021D04), and the Key Research and Development Project of Yunnan Province (grant number 202003AC100002). Key Research and Development Plan of Yunnan Province (202203AC100003).

## CRediT authorship contribution statement

**Jie Liu:** Writing – review & editing, Supervision, Funding acquisition. **Yi Chen:** Writing – original draft, Software. **Wanqing Wang:** Writing – review & editing. **Chenwei Hao:** Validation. **Fei Cai:** Investigation. **Liangyun Teng:** Investigation. **Xuehua Luo:** Software.

## Declaration of competing interest

The authors declare that they have no known competing financial interests or personal relationships that could have appeared to influence the work reported in this paper.

## Acknowledgements

I would like to express my sincere gratitude to the following individuals for their support and assistance throughout the completion of this thesis.

Firstly, I am deeply grateful to my supervisor, Jie Liu, whose patient guidance and expert advice have enabled me to progress steadily through the research, overcoming numerous challenges along the way. I would also like to thank all the members of the laboratory, especially chenwei Hao, xuehua Luo, cai Fei and liangyun Teng for their collaboration, sharing valuable insights and experiences that have provided crucial support to this study. Lastly, my heartfelt thanks go to my family and friends, who have consistently supported and encouraged me throughout my graduate studies, offering endless love and understanding.

## References

- [1] Chuangen Hou, Haiming Yu, Yuxi Ye, Xianhang Yang, Yuhuan Wang, Weimin Cheng Study on dust pollution characteristics and optimal dust control parameters during tunnel excavation by CFD simulation, *Adv. Powder Technol.* 34 (Issue 11) (2023), 104217ISSN 0921-8831.
- [2] Changqi Liu, Bao Qiu, Nie Wen, The influence of ventilation parameters on dust pollution in a tunnel's environment using the CFD method, *J. Wind Eng. Ind. Aerod.* 230 (2022) 105173. ISSN 0167-6105.
- [3] Lianjun Chen, Guoming Liu, Airflow-dust migration law and control technology under the simultaneous operations of shotcreting and drilling in roadways, *Arabian J. Sci. Eng.* 44 (5) (2019).
- [4] Nie Wen, Wenle Wei, Xiao Ma, Yanghao Liu, Huitian Peng, Qiang Liu, The effects of ventilation parameters on the migration behaviors of head-on dusts in the heading face, *Tunn. Undergr. Space Technol.* 70 (2017) 400–408. ISSN 0886-7798.
- [5] Zhiwei Hu, Jianyi Bi, Haidong Wang, Study on the transport law of blasting dust in long-distance digging face of Xiaogou coal mine, *China Mining Industry* 28 (S2) (2019) 340–345.
- [6] Wei Niu, Zhongan Jiang, Tian Dongmei, Numerical simulation of the factors influencing dust in drilling tunnels: its application, *Min. Sci. Technol.* 21 (1) (2011) 11–15. ISSN 1674-5264.
- [7] Cai Xiaojiao, Nie Wen, Yin Shuai, et al., An assessment of the dust suppression performance of a hybrid ventilation system during the tunnel excavation process: numerical simulation, *Process Saf. Environ. Protect* (1) (2021) 304–317 (prepublish) ISSN 0957-5820.
- [8] Jiang Zhong-an, Ya-peng Wang, Li-guo Men, Ventilation Control of Tunnel Drilling Dust Based on Numerical Simulation, *Journal of Central South University*, 2021 (prepublish).
- [9] Yimin Xia, Duan Yang, Chenghuan Hu, Caizhang Wu, Jialin Han, Numerical simulation of ventilation and dust suppression system for open-type TBM tunneling work area, *Tunn. Undergr. Space Technol.* 56 (2016) 70–78. ISSN 0886-7798.
- [10] Jundika Candra Kurnia, Agus Pulung Sasmito, Arun Sadashiv Mujumdar, Dust dispersion and management in underground mining faces, *Int. J. Min. Sci. Technol.* 24 (1) (2014) 39–44. ISSN 2095-2686.
- [11] Ronghua Liu, Haiqiao Wang, Shiliang Shi, et al., Study on the distribution law of flour dust in press-in ventilated tunneling, *J. China Coal Soc.* (3) (2002) 233–236.
- [12] Haiqiao Wang, Shiliang Shi, Ronghua Liu, et al., Numerical simulation study of the air flow field of the jet flow with the wall of the single-headed roadway, *J. China Coal Soc.* (4) (2004) 425–428.
- [13] Haiqiao Wang, Study on the air flow field of the jet flow at the excavation face, *J. China Coal Soc.* (5) (1999) 498–501.
- [14] J. Torano, S. Torno, M. Menéndez, M. Gent, Auxiliary ventilation in mining roadways driven with roadheaders: validated CFD modelling of dust behaviour, *Tunn. Undergr. Space Technol.* 26 (1) (2011) 201–210. ISSN 0886-7798.
- [15] Agus P. Sasmito, Erik Birgersson, Hung C. Ly, Arun S. Mujumdar, Some approaches to improve ventilation system in underground coal mines environment-A computational fluid dynamic study, *Tunn. Undergr. Space Technol.* 34 (2013) 82–95. ISSN 0886-7798.
- [16] Changqi Liu, Nie Wen, Qiu Bao, Qiang Liu, Cunhou Wei, Yun Hua, The effects of the pressure outlet's position on the diffusion and pollution of dust in tunnel using a shield tunneling machine, *Energy Build.* 176 (2018) 232–245. ISSN 0378-7788.
- [17] Zhongqiang Sun, Research on the Law and Control Technology of Dust Migration in the Construction of Highway Tunnel Drilling and Blasting Method, *University of Science and Technology Beijing*, 2015.
- [18] Lidian Guo, Nie Wen, Shuai Yin, Qiang Liu, Yun Hua, Lei Cheng, Xiaojiao Cai, Zihao Xiu, Tao Du, The dust diffusion modeling and determination of optimal airflow rate for removing the dust generated during mine tunneling, *Build. Environ.* 178 (2020) 106846. ISSN 0360-1323.
- [19] Qiang Liu, Nie Wen, Yun Hua, Huitian Peng, Changqi Liu, Cunhou Wei, Research on tunnel ventilation systems: dust Diffusion and Pollution Behaviour by air curtains based on CFD technology and field measurement, *Build. Environ.* 147 (2019) 444–460. ISSN 0360-1323.
- [20] Kefu Yao, Shiguang Tian, et al., Research progress on the service performance of concrete dams driven by the characteristic environment in high altitude areas, *J. Hydraul. Eng.* 54 (6) (2023) 717–728, <https://doi.org/10.13243/j.cnki.slxb.20221013>.